Z. Phys. C – Particles and Fields 41, 557–566 (1989)

Zeitschrift für Physik C Particles and Fields

Inclusive ϕ-meson production in electron-positron interactions in the energy region of the Υ-resonances

ARGUS Collaboration

H. Albrecht, P. Böckmann, R. Gläser, G. Harder, A. Krüger, A. Nippe, M. Schäfer, W. Schmidt-Parzefall, H. Schröder, H.D. Schulz, F. Sefkow, J. Spengler, R. Wurth, A. Yagil
DESY, Hamburg, Federal Republic of Germany

R.D. Appuhn, A. Drescher, D. Kamp, H. Kolanoski, R. Mankel, U. Matthiesen, H. Scheck, G. Schweda, B. Spaan, A. Walther, D. Wegener
Institut für Physik[1], Universität, Dortmund, Federal Republic of Germany

J.C. Gabriel, T. Ruf, S. Schael, K.R. Schubert[2], J. Stiewe, K. Strahl, R. Waldi, S. Werner
Institut für Hochenergiephysik[3], Universität, Heidelberg, Federal Republic of Germany

K.W. Edwards[4], W.R. Frisken[5], H. Kapitza[4], R. Kutschke[6], D.B. MacFarlane[7], K.W. McLean[7], A.W. Nilsson[7], R.S. Orr[6], J.A. Parsons[6], P.M. Patel[7], J.D. Prentice[6], S.C. Seidel[6], J.D. Swain[6], G. Tsipolitis[7], T.-S. Yoon[6]
Institute of Particle Physics[8], Canada

R. Ammar, S. Ball, D. Coppage, R. Davis, S. Kanekal, N. Kwak
University of Kansas[9], Lawrence, Kan., USA

B. Boštjančič, G. Kernel, P. Križan, E. Križnič, M. Pleško
Institut J. Stefan and Oddelek za fiziko[10], Univerza v Ljubljani, Ljubljana, Yugoslavia

H.I. Cronström, L. Jönsson
Institute of Physics[11], University of Lund, Sweden

A. Babaev, M. Danilov, B. Fominykh, A. Golutvin, I. Gorelov, V. Lubimov, V. Matveev, A. Semenov, S. Semenov, V. Shevchenko, V. Soloshenko, V. Tchistilin, I. Tichomirov, Yu. Zaitsev
Institute of Theoretical and Experimental Physics, Moscow, USSR

R. Childers, C.W. Darden, R.C. Fernholz
University of South Carolina[12], Columbia, SC, USA

Received 18 July 1988; in revised form 26 September 1988

Abstract. We report on a high precision measurement of ϕ-meson production in continuum events and in direct decays of the $\Upsilon(1S)$- and $\Upsilon(2S)$-mesons. The ratio of the total production rate of ϕ-mesons in direct $\Upsilon(1S)$- and $\Upsilon(2S)$-decays over that in continuum events is $1.32 \pm 0.08 \pm 0.09$ and $1.07 \pm 0.13 \pm 0.11$ respectively. This is compatible with the corresponding ratio obtained for lighter mesons, but is appreciably smaller than the relative baryon production rate.

1 Introduction

High statistics studies of meson production in the fragmentation of partons produced in electron-posi-

[1] Supported by the German Bundesministerium für Forschung und Technologie, under contract number 054DO51P
[2] Now at Institut für Experimentelle Kernphysik, Universität Karlsruhe
[3] Supported by the German Bundesministerium für Forschung und Technologie, under contract number 054HD24P
[4] Carleton University, Ottawa, Ontario, Canada
[5] York University, Downsview, Ontario, Canada
[6] University of Toronto, Toronto, Ontario, Canada
[7] McGill University, Montreal, Quebec, Canada
[8] Supported by the Natural Sciences and Engineering Research Council, Canada
[9] Supported by the U.S. National Science Foundation
[10] Supported by Raziskovalna skupnost Slovenije and the Internationales Büro KfA, Jülich
[11] Supported by the Swedish Research Council
[12] Supported by the U.S. Department of Energy, under contract DE-AS09-80ER10690

tron interactions have been, up to now, confined to light stable mesons [1]. Such studies suffer from the limitation that light mesons are predominantly the decay products of heavier resonances. Hence, these measurements provide only second-hand information about the fragmentation process. For example, the search for scale-breaking effects is severely hampered by the softening of the particle spectrum due to resonance decays, which can simulate part of the scale-breaking effect. Decays of heavy hadrons can only be corrected for by detailed modelling of the fragmentation process. Hence, systematic uncertainties cannot be avoided as long as the production of heavier resonances is not sufficiently understood. Scale breaking effects in the momentum spectrum of heavier particles, such as ϕ-mesons, should not suffer from these limitations, since ϕ-mesons are not common decay products of heavier resonances [2], and, in cases where they are, most of the parent momentum will be passed to the ϕ-mesons due to their large mass.

Since the ϕ-meson is nearly a pure $s\bar{s}$-state, a comparison of production rates with that of mesons with only one strange valence quark allows the direct determination of the $SU(3)$ breaking of the quark sea [3]. K^*-mesons are, in this context, particularly suitable since their mass is only slightly smaller. Therefore mass effects – which influence hadron production in the fragmentation process – are expected to be small.

A comparison of the ϕ-meson rate observed in direct $\Upsilon(1S)$ decays with the corresponding rate in the continuum is also of considerable interest. This measurement allows a check of the conjecture [4] that the observed enhancement of baryon production in direct $\Upsilon(1S)$ decays over that in the continuum can be traced back to the production of higher mass clusters in the resonance decays [5]. ϕ-meson production in direct $\Upsilon(1S)$ decays should, in addition, be even less influenced by resonance decays than the continuum, since the latter includes contributions from charmed meson decays [6]. This source is negligible in direct $\Upsilon(1S)$ decays [7].

Finally, it should be noted that ϕ-mesons, as isosinglet states, have been cited as preferential gluon fragmentation products [8]. Hence, studies of ϕ-meson production promise to shed light on the intriguing problem of differences between quark and gluon fragmentation.

2 Data analysis

2.1 Data sample

The data used in the analysis reported here were collected with the ARGUS detector at the DORIS II storage ring at DESY. The event sample corresponds to an integrated luminosity of 25.7 pb^{-1} on the $\Upsilon(1S)$, 18.0 pb^{-1} on the $\Upsilon(2S)$ and 37.0 pb^{-1} in the continuum. The ARGUS detector is a 4π spectrometer described in more detail in [9]. The momenta of charged particles and their mean energy loss were measured using the ARGUS drift chamber. The mass of particles was determined using both specific ionization and time-of-flight measurements. A description of the particle identification procedure can be found in [7].

2.2 Event selection

The detector triggers not only on multihadron events produced in e^+e^- annihilation and direct decays of the Υ-resonances, but also on backgrounds from QED events, such as lepton pair production, from beam-gas and beam-wall interactions and from two-photon events. These backgrounds are reduced to a negligible level by applying the following cuts:

- $\geqq 3$ charged tracks are reconstructed with a common vertex lying within a radius $r < 1.5$ cm and a longitudinal distance $|z| < 6$ cm of the nominal interaction point.
- Beam-wall, beam-gas and $\gamma\gamma$-events can be distinguished from multihadron events by comparing the sum of the scalar momentum of the charged and neutral particles

$$P_{\text{sum}} = \frac{\sum_i |\mathbf{p}_i|}{\sqrt{s}}$$

with the sum of the momentum component along the beam line

$$P_z = \frac{\sum_i p_{z_i}}{\sqrt{s}}.$$

The cut

$$P_{\text{sum}} \geqq 0.4 + 2.5 P_z^2$$

effectively rejects all these background events (Fig. 1a) while retaining nearly all multihadron events.
- As demonstrated by Fig. 1b, after these cuts a background remains from radiative QED processes where the photon converts. This background can be rejected by requiring, in addition, at least two photons detected in the calorimeter.

The efficiency for multihadron events to pass all these cuts was found by a Monte Carlo calculation, including a detailed detector simulation [10], to vary from 80% to 94% depending on the type of event ($q\bar{q}$, ggg, ...). Details are discussed in Sect. 2.4. From

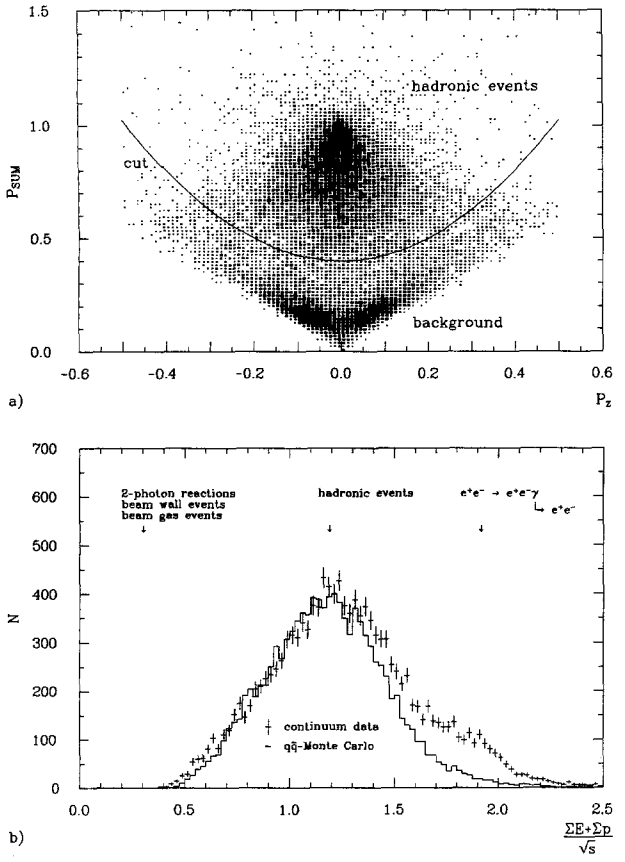

Fig. 1a, b. Reduction of background by applying the $P_{sum}-P_z$ cut. **a** The cut in the $P_{sum}-P_z$ plane (data from continuum). **b** Sum of momenta of all charged particles and the total energy deposited in the calorimeter scaled by the center-of-mass energy after the cut. The rejection of the remaining QED background is described in the text

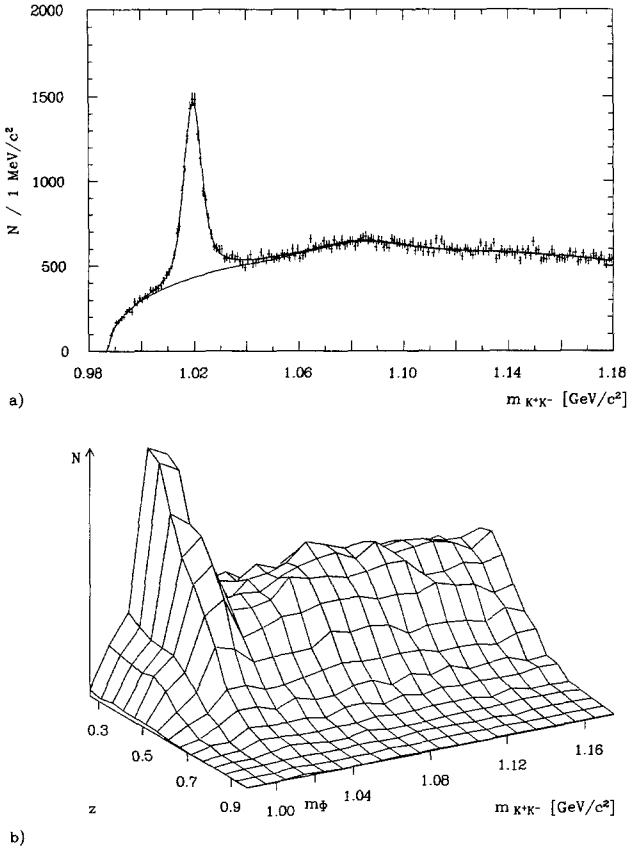

Fig. 2. a Invariant mass distribution of all K^+K^- candidates from resonances and continuum. The function used for the fit shown consists of a convolution of a relativistic p-wave Breit-Wigner distribution with a Gaussian for the signal, a Gaussian for the reflection from the K^* decay and a 2nd order polynomial multiplied by a phase space factor for the background. **b** Scaled energy z of candidates vs. their invariant mass

an analogous treatment of simulated τ-pairs and the knowledge of their production cross section the contamination of the continuum data by events of this type was determined to be 3% and was corrected for in the analysis. The remaining background after these cuts was estimated to be less than 1%.

2.3 Determination of the ϕ-signal

The invariant mass distribution of K^+K^- pairs exhibits a prominent peak at the mass of the ϕ-meson (Fig. 2a) above a smooth background. As demonstrated by Fig. 2b, the signal is most pronounced at small values of the scaled energy

$$z=\frac{2E_\phi}{\sqrt{s}}$$

of the ϕ-meson, but does extend up to the kinematic limit. Since the shape of the z distribution for the non-resonant background is independent of the invariant mass of the K^+K^- system, as demonstrated for two particular mass intervals in Fig. 3a, a sideband subtraction method was used to determine the ϕ-spectrum. This method has the technical advantage that the free parameters describing the background and the signal are determined only once, with high precision, for the K^+K^- invariant mass distribution integrated over all z values.

The sideband signal was determined in the two mass intervals

$$0.990\ \text{GeV/c}^2 \leqq m_{K^+K^-} < 1.005\ \text{GeV/c}^2$$
$$1.040\ \text{GeV/c}^2 \leqq m_{K^+K^-} < 1.055\ \text{GeV/c}^2.$$

This choice excludes contributions due to misidentified e^+e^--pairs from photon conversion and reflections of the K^{*0} signal (Fig. 3b). Technical details of the sideband subtraction are discussed in [11].

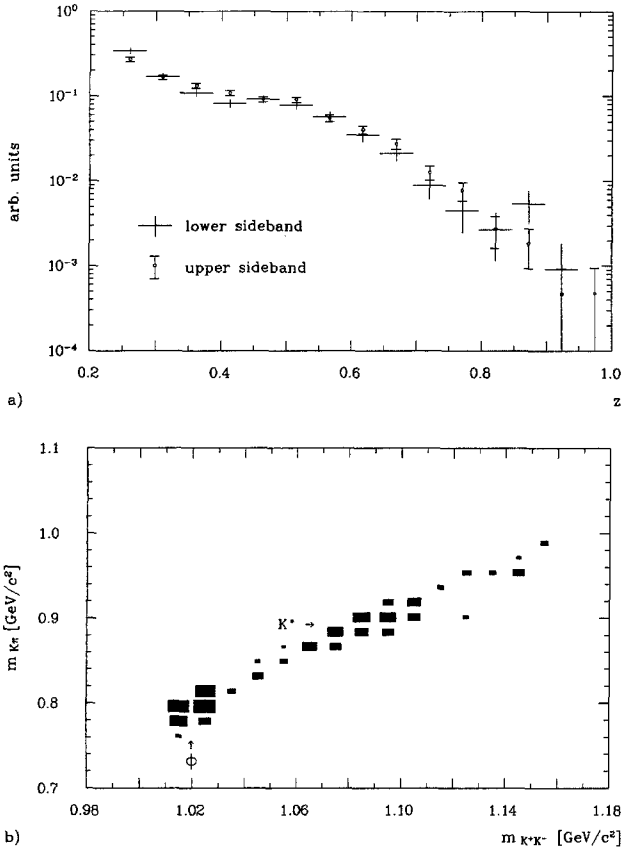

Fig. 3. a Comparison of lower and upper sideband (data from $\Upsilon(1S)$). **b** Influence of ambiguous particle identification. Shown are cases in which one of the two particles forming a ϕ-candidate could be identified as K or π. For clarity, bins with less than 250 entries are not displayed. The invariant mass of the reflection from the K^* is reliably separated from the ϕ-mass

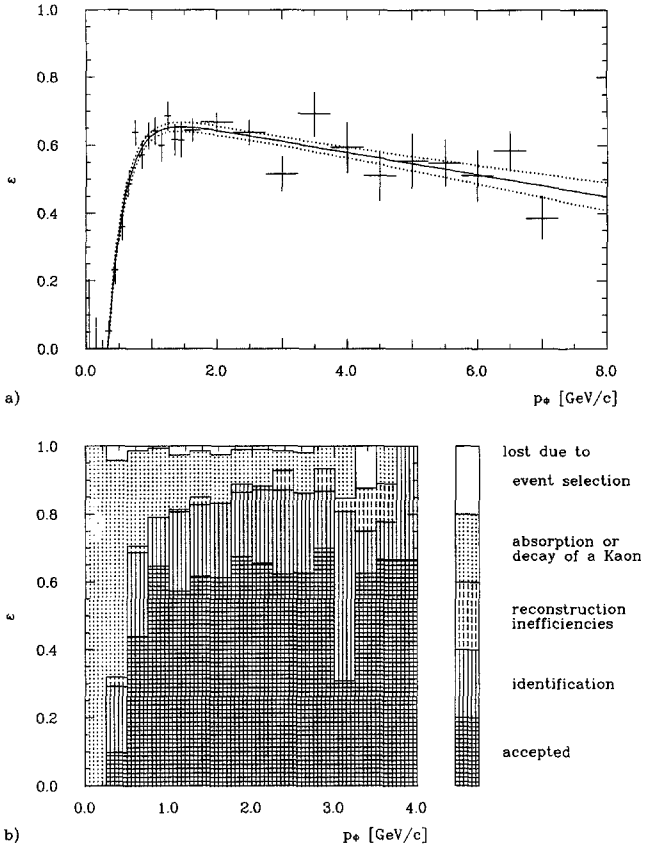

Fig. 4 a, b. Momentum dependence of efficiency of ϕ meson reconstruction. **a** The solid line represents the fit result to combined data (crosses) from $q\bar{q}$-, 3-gluon and phase space Monte Carlo. The error of the fit is given by the dotted lines. **b** Different sources of inefficiency ($q\bar{q}$ Monte Carlo events)

2.4 Acceptance calculations

The efficiency for multihadron events to pass the cuts discussed in Sect. 2.2 was determined by means of a Monte Carlo calculation. Events of the type $e^+e^- \to q\bar{q}(\gamma)$ and $\Upsilon(1S) \to ggg$ were generated using JETSET version 6.2 [12], an event generator based on the Lund string model [13]. These events were then passed through a detailed detector simulation [10]. The same cuts were applied as for the data. Since the efficiencies for multihadron events depend slightly on the parton configuration of the final state, a proper mixture was chosen for every energy. The results are summarized in Table 1.

The ϕ-meson reconstruction efficiency was derived from the same Monte Carlo calculation. This turned out to only depend on the momentum of the ϕ-meson (Fig. 4 a) and was insensitive to the topological configuration of the final state. In Fig. 4 b the different sources of efficiency loss and their momentum dependence are displayed. Low momentum

Table 1. Mixture of event types for different energy classes

	$q\bar{q}$	ggg	gg	$q\bar{q}g$[a]
ε [%]	80±2	94±2	87±7	87±7
Class	Mixture of event types [%]			
$\Upsilon(1S)$	10.2	89.8		
$\Upsilon(2S)$	9.7	75.3	10.2	4.8
Continuum	100			

[a] The only contribution to this column is the decay of the χ_{b1} [14]

$K^\pm$-mesons are mainly lost due to decay in flight. The slight decrease of the efficiency at high momenta can be explained by an increased overlap of high momentum $K^\pm$-mesons from the ϕ-decay, which results in a decrease in the reconstruction efficiency due to ambiguous wire assignment during the track finding procedure. The effect of the cut on the polar angle

of the ϕ-meson at $|\cos\theta| < 0.7$ depends on the topology of the event. The efficiency of the cut is 0.689 ± 0.006 for the 3-gluon decays and 0.647 ± 0.006 for $q\bar{q}$ pairs. The errors include uncertainties in the angular distribution of tracks caused by the event generator.

2.5 *Determination of the inclusive particle spectra*

The continuum spectrum is derived from the acceptance corrected rates using the measured luminosity. The softening of the particle spectrum due to radiative effects was taken into account using the Lund Monte Carlo program [12], including the contributions of ψ and Υ states produced through initial state radiation. The influence of the radiative corrections on the slope of the spectrum is demonstrated by Fig. 5.

Of particular interest is the differential cross section for decays of the Υ-meson into hadrons excluding the contribution from the vacuum polarization diagram. The latter is obtained from the measured continuum cross section corrected for radiative effects:

$$\frac{d\sigma_{\text{vac}}}{dz} = \frac{B_{\mu\mu}\,\sigma_{\text{res}\to\text{had}}}{(1-3B_{\mu\mu})\,\sigma^0_{e^+e^-\to\mu^+\mu^-}} \cdot \frac{d\sigma^0_{\text{cont}\to\text{had}}}{dz}$$

with

$B_{\mu\mu}$ branching ratio for decay $\Upsilon \to \mu^+\mu^-$

$\frac{d\sigma^0_{\text{cont}\to\text{had}}}{dz}$ differential continuum cross section for hadron production. The superscript 0 denotes a cross section in lowest order QED.

$\sigma^0_{e^+e^-\to\mu^+\mu^-}$ cross section for $\mu^+\mu^-$-pair production in e^+e^--reactions in lowest order QED.

$\sigma_{\text{res}\to\text{had}}$ $= \sigma_{\text{had}} - \sigma_{\text{cont}\to\text{had}}$.

σ_{had} production cross section of hadrons measured at the resonance energy, including resonance and continuum contributions.

$\sigma_{\text{cont}\to\text{had}}$ continuum cross section measured at the resonance energy.

The last quantity is derived from the cross section measured at a nearby continuum energy $\sqrt{s_{\text{cont}}}$, by rescaling the point-like cross section for quark-pair production in e^+e^- reactions according to

$$\sigma^0_{\text{cont}\to\text{had}}(s_{\text{res}}) = \frac{s_{\text{cont}}}{s_{\text{res}}} \cdot \sigma^0_{\text{cont}\to\text{had}}(s_{\text{cont}})$$

and taking into account the energy dependence of radiative effects.

Combining all contributions, one obtains for the cross section for direct resonance decays

$$\frac{d\sigma_{\text{dir}}}{dz} = \frac{d\sigma_{\text{had}}}{dz} - \frac{d\sigma_{\text{cont}\to\text{had}}}{dz} - \frac{d\sigma_{\text{vac}}}{dz}.$$

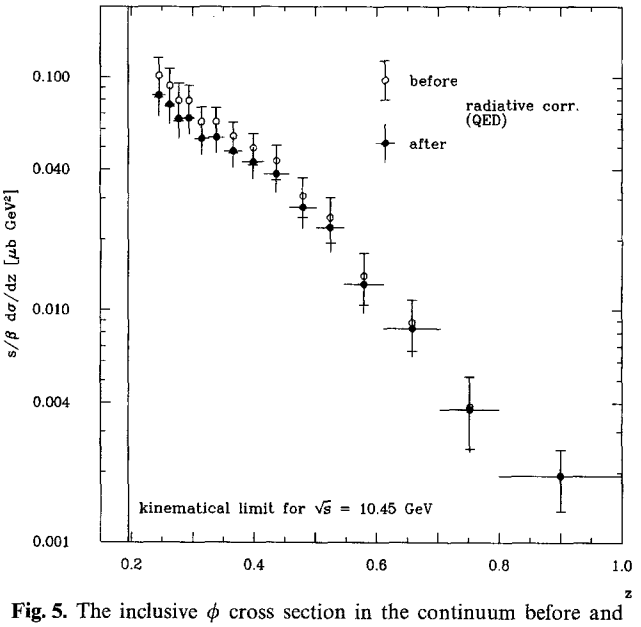

Fig. 5. The inclusive ϕ cross section in the continuum before and after applying radiative corrections

In the following discussion the differential particle densities, and not the differential cross sections, are often of interest. If N_{had} is the number of hadronic events, the two distributions are easily related for continuum data:

$$\frac{1}{N_{\text{had}}}\frac{dn}{dz} = \frac{1}{\sigma_{\text{cont}\to\text{had}}}\frac{d\sigma}{dz}.$$

No simple expression holds for direct resonance decays, since the effective total resonance cross section depends on the energy resolution of the storage ring.

For these and all subsequent calculations the following sources of systematic error were taken into account:

- Uncertainties in computing the non-radiative continuum spectrum (2%).
- Differences between the different data samples due to instabilities of detector behaviour and luminosity determination (1% each).
- On resonance, the uncertainty of $B_{\mu\mu}$, which enters the calculation in the continuum subtraction as $(2.78 \pm 0.22)\%$ for the $\Upsilon(1S)$ and $(1.80 \pm 0.44)\%$ for the $\Upsilon(2S)$ respectively [2].
- Momentum dependent errors in the efficiency for ϕ-mesons (typically 2.5%).
- Uncertainties in determining the number of hadronic events (depending on the class of data, typically 3%).
- The error on the branching ratio of the decay channel $\phi \to K^+K^-$ (3%). This contribution cancels in determination of the ratio of production rates on Υ and in the continuum.

- The uncertainty of the luminosity scale has in addition been considered when calculating the differential cross section instead of production rates (3%).

Since the above sources of systematic errors are uncorrelated their contributions were added in quadrature.

3 Results and comparison with model predictions

3.1 Continuum data

The measured inclusive cross section is plotted in Fig. 6 and listed in Table 2 for the continuum data. The energy dependence of the production cross section for two pointlike fermions in e^+e^- interactions and the threshold behaviour of the scaling cross section are accounted for by multiplying $d\sigma/dz$ by a factor s/β. Hence the present analysis can be directly compared with other experimental results included in Fig. 6. The width of the z interval contributing to each data point is indicated by the horizontal bar in those cases where it is has been given. Note that the minimum value allowed for z

$$z_{\text{th}}=\frac{2m_\phi}{\sqrt{s}}$$

is energy dependent. Within errors, the results from the different experiments agree.

In Fig. 7 the normalized differential particle density

$$g(z)=\frac{1}{\beta}\frac{1}{N_{\text{had}}}\frac{dn}{dz}=\frac{1}{\beta}\frac{1}{\sigma_{\text{cont}\to\text{had}}}\frac{d\sigma}{dz}$$

Table 2. The differential cross section for ϕ-production in the continuum after applying radiative corrections

z interval	$\frac{s}{\beta}\frac{d\sigma}{dz}$ [μb GeV^2]
0.235–0.255	0.084 $\pm$0.016 $\pm$0.005
0.255–0.270	0.076 $\pm$0.014 $\pm$0.005
0.270–0.285	0.066 $\pm$0.012 $\pm$0.004
0.285–0.303	0.066 $\pm$0.011 $\pm$0.004
0.303–0.326	0.0544 $\pm$0.0087 $\pm$0.0032
0.326–0.351	0.0550 $\pm$0.0081 $\pm$0.0032
0.351–0.381	0.0479 $\pm$0.0074 $\pm$0.0028
0.381–0.416	0.0431 $\pm$0.0067 $\pm$0.0025
0.416–0.457	0.0383 $\pm$0.0064 $\pm$0.0023
0.457–0.502	0.0275 $\pm$0.0053 $\pm$0.0016
0.502–0.547	0.0225 $\pm$0.0049 $\pm$0.0013
0.547–0.612	0.0129 $\pm$0.0032 $\pm$0.0008
0.612–0.704	0.0083 $\pm$0.0021 $\pm$0.0005
0.704–0.800	0.0037 $\pm$0.0013 $\pm$0.0002
0.800–1.000	0.0019 $\pm$0.0006 $\pm$0.0001

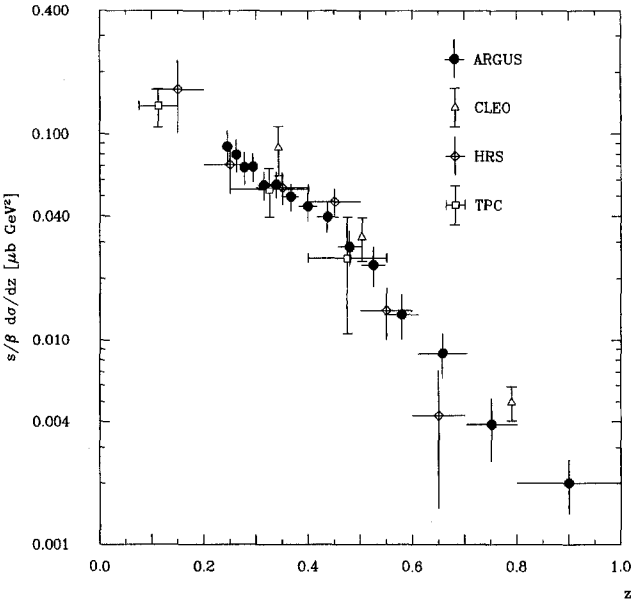

Fig. 6. Comparison of the measured ϕ continuum cross section with other experiments [20–22]

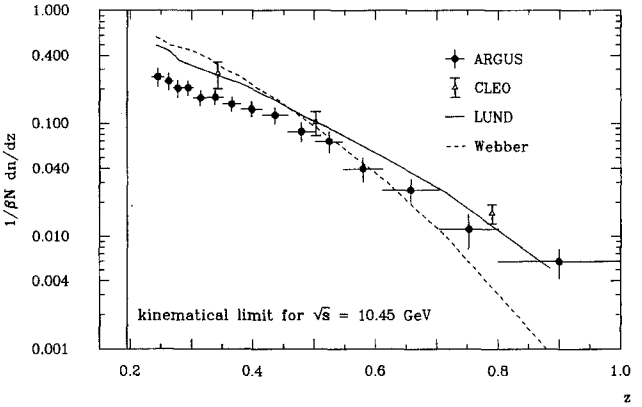

Fig. 7. Comparison of the differential particle density in the continuum with CLEO [20] and model predictions

is compared to predictions based on the string [13] and parton shower models [15, 16]. Version 6.2 of the Lund string model was used, while for the parton shower model the parameters tuned by Ng [17] were taken, with the exception of the parameter describing the $SU(3)$ breaking for sea quarks in gluon splitting. This last was set to the standard value of 0.3, instead of modifying the parameters controlling the cluster decay [18]. The models reproduce neither the shape nor the normalization of the measured spectrum. The rates predicted by the parton shower model at low z are approximately a factor of two higher than the measurement, while at large z the model underestimates the rates. The latter effect has already been observed for stable particles [19] and has been traced

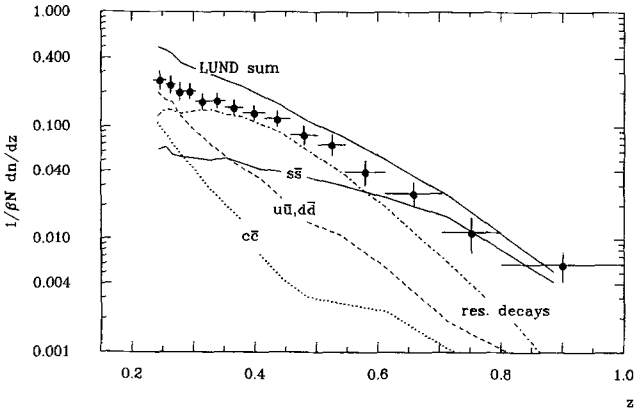

Fig. 8. Comparison of continuum data with the prediction of the LUND model. The contributions to the total prediction are divided into the various sources of ϕ-mesons: direct production in the fragmentation of different leading quarks and resonance decays

back to the fact that all colour singlet clusters are forced to decay into at least two particles.

In order to examine in more detail the source of the deviation between the predictions of the string model [12] and the data, the different sources of ϕ-mesons are plotted separately in Fig. 8. Along with those ϕ-mesons produced in jets by a leading $u\bar{u}$-, $d\bar{d}$- and $s\bar{s}$-quark pair, the contribution of c-quark fragmentation is also shown. The latter is divided into a fragmentation contribution and a resonance contribution from the weak decay of charmed mesons. Since the inclusive branching ratios of $D^{\pm}$-, D^0- and D_s-meson decays into ϕ-mesons are not all known experimentally, these must be considered as free parameters of the model. The fact that this contribution alone saturates the measured cross section at $z \sim 0.35$ indicates that the inclusive branching ratio for charmed mesons decays into ϕ-mesons is smaller than assumed in the model. This conclusion will be substantiated by the results following from direct $\Upsilon(1S)$-decays.

3.2 Direct Υ-decays

The inclusive spectra of ϕ-mesons produced in direct decays of the $\Upsilon(1S)$- and $\Upsilon(2S)$-meson are plotted in Fig. 9 a, b and listed in Tables 3 and 4. In both cases the particle densities are given. It is tempting to compare the two spectra, since three gluon decays should dominate the final state in both cases. As demonstrated by Fig. 9 c the two do indeed coincide within errors.

In Fig. 10 the result of the present analysis for direct $\Upsilon(1S)$-decays is compared to data published by the CLEO collaboration [20]. The CLEO spetrum is somewhat softer than the ARGUS results. The prediction of the Lund string [12] and the parton shower model [16] are included for comparison. Note that the agreement between data and model predictions is better than for the continuum data. This observation sustains the conclusions drawn in Sect. 3.1 that the discrepancies observed for continuum data are mainly due to excessively large inclusive branching ratios for charmed meson decays into ϕ-mesons assumed in the Lund model, since the production of charmed mesons in direct $\Upsilon(1S)$-decays is known experimentally to be suppressed [7]. Note however that at medium $z \approx 0.5$ the experimental data are a factor of 2.5 larger than the model predictions.

Table 3. The differential particle density $1/(\beta N_{\text{had}})\, dn_\phi/dz$ for inclusive ϕ-production in direct decays of the $\Upsilon(1S)$

z interval	$\frac{1}{\beta N}\frac{dn}{dz}$
0.235–0.255	0.711 ±0.088 ±0.057
0.255–0.270	0.597 ±0.071 ±0.036
0.270–0.285	0.496 ±0.060 ±0.026
0.285–0.303	0.384 ±0.046 ±0.019
0.303–0.326	0.372 ±0.037 ±0.018
0.326–0.351	0.233 ±0.030 ±0.012
0.351–0.381	0.171 ±0.025 ±0.009
0.381–0.416	0.101 ±0.020 ±0.006
0.416–0.457	0.081 ±0.018 ±0.005
0.457–0.502	0.066 ±0.016 ±0.004
0.502–0.547	0.055 ±0.014 ±0.003
0.547–0.612	0.036 ±0.009 ±0.002
0.612–0.704	0.0068 ±0.0053 ±0.0007
0.704–0.800	0.0068 ±0.0034 ±0.0005
0.800–1.000	−0.0005 ±0.0012 ±0.0002

Table 4. The differential particle density $1/(\beta N_{\text{had}})\, dn_\phi/dz$ for inclusive ϕ-production in direct decays of the $\Upsilon(2S)$

z interval	$\frac{1}{\beta N}\frac{dn}{dz}$
0.235–0.255	0.68 ±0.15 ±0.05
0.255–0.270	0.60 ±0.14 ±0.04
0.270–0.285	0.39 ±0.11 ±0.03
0.285–0.303	0.257 ±0.092 ±0.018
0.303–0.326	0.207 ±0.073 ±0.015
0.326–0.351	0.293 ±0.068 ±0.019
0.351–0.381	0.112 ±0.053 ±0.010
0.381–0.416	0.039 ±0.045 ±0.007
0.416–0.457	0.077 ±0.042 ±0.008
0.457–0.502	−0.001 ±0.032 ±0.004
0.502–0.547	0.041 ±0.030 ±0.004
0.547–0.612	0.021 ±0.019 ±0.002
0.612–0.704	−0.004 ±0.011 ±0.001
0.704–0.800	−0.0083 ±0.0061 ±0.0006
0.800–1.000	−0.0041 ±0.0023 ±0.0003

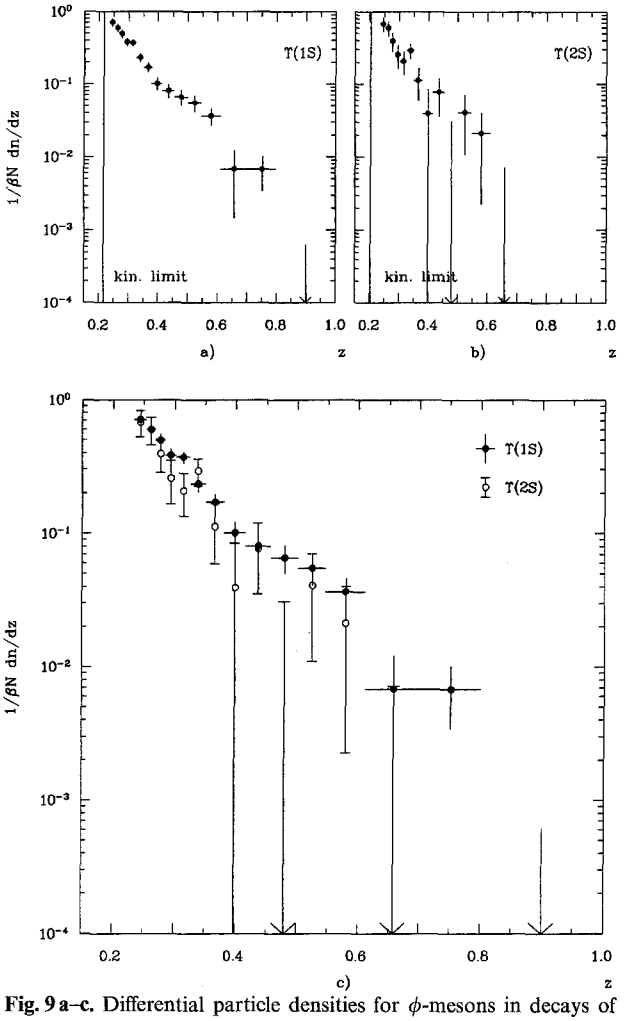

Fig. 9 a–c. Differential particle densities for ϕ-mesons in decays of Υ-mesons. **a** Data from direct $\Upsilon(1S)$ decays, **b** data from direct $\Upsilon(2S)$ decays, **c** both overlayed

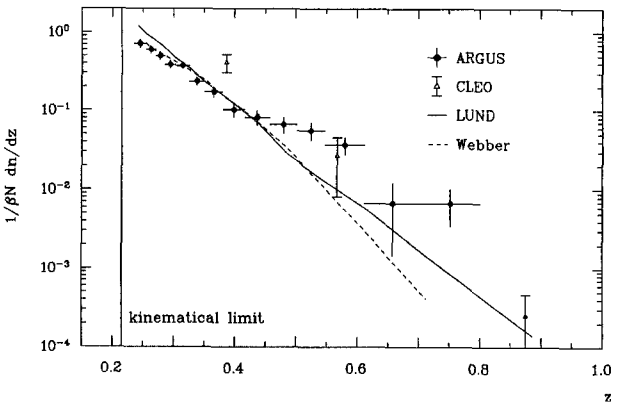

Fig. 10. Differential particle density for ϕ-production in direct $\Upsilon(1S)$-decays compared with model predictions and measurements from CLEO [20]

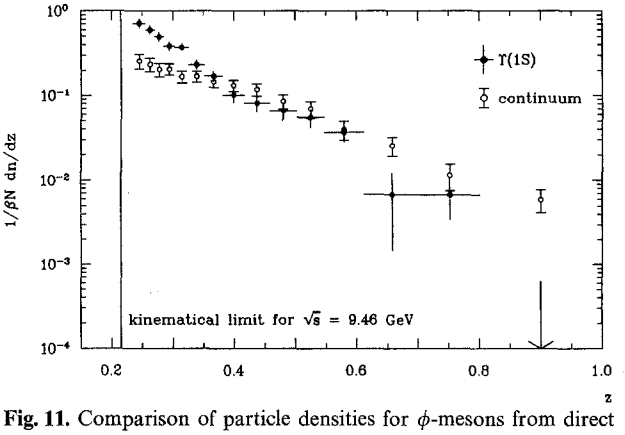

Fig. 11. Comparison of particle densities for ϕ-mesons from direct decays of the $\Upsilon(1S)$ and from the continuum

3.3 Comparison of ϕ-meson production in direct Υ-decays with continuum data

The measured particle densities $g(z)$ for direct $\Upsilon(1S)$-decays and for continuum events are compared in Fig. 11. As previously observed for stable particles [20], the spectrum for direct Υ-decays decreases faster with increasing z than the corresponding continuum data. This result is not surprising since these decays are expected to proceed via three-gluon emission by the $b\bar{b}$ state, while the continuum data are due to $q\bar{q}$ production. Fragments in the latter case can therefore take a larger fraction of the total energy, resulting in a flatter spectrum.

As pointed out in Sect. 1, the comparison of the total number of ϕ-mesons in the three-gluon decay with the corresponding number from continuum fragmentation is of special interest, since parton shower models predict this ratio

$$r = \frac{\#\text{ of hadrons per direct } \Upsilon\text{-decay}}{\#\text{ of hadrons per continuum event}}$$

will increase with the mass of the particle considered. This behaviour is claimed [5] to explain the large experimental value for r observed for baryons but not for mesons [20, 23, 24]. In Table 5 the numbers of ϕ-mesons produced per event in direct $\Upsilon(1S)$-, $\Upsilon(2S)$-decays and in the continuum are summarized. These are derived from the experimental data by integrating the particle densities:

$$\langle n_\phi \rangle = \int_{z_{th}}^{1} g(z) \cdot \beta(z)\, dz.$$

Assuming a scaling behaviour for $g(z)$, which certainly holds for the energy range covered by this experiment, this expression allows a determination of the produc-

Table 5. Measured and predicted rates of ϕ-meson production in resonance decays and in the continuum

	Res. energy	Res. decays	Cont. at res. energy
ARGUS	$\Upsilon(1S)$	$0.0545 \pm 0.0022 \pm 0.0034$	$0.0413 \pm 0.0020 \pm 0.0021$
	$\Upsilon(2S)$	$0.0481 \pm 0.0051 \pm 0.0049$	$0.0448 \pm 0.0021 \pm 0.0024$
LUND 6.2	9.46	0.0651 ± 0.0005	0.0731 ± 0.0006
Webber	9.46	0.0531 ± 0.0005	0.0829 ± 0.0007

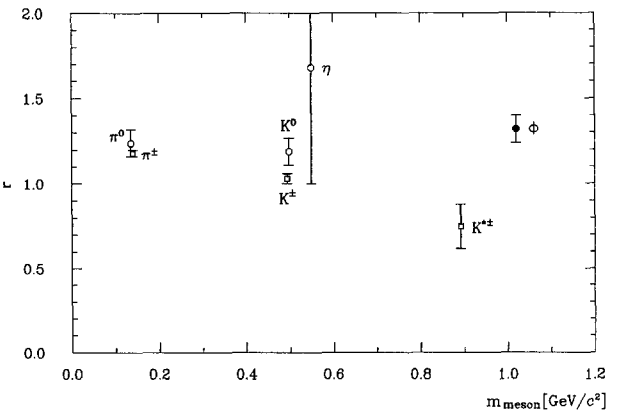

Fig. 12. The ratio of production rates ($\Upsilon(1S)$/cont) for several mesons [25–28]. For baryons, one obtains values of 2.5–3.5 [24]

tion rates in the continuum at different center-of-mass energies by modifying $z_{\text{th}}(\sqrt{s})$ and $\beta(z, \sqrt{s})$ appropriately. Note that in this experiment data are available for $z_{\min} \geqq 0.235$. Therefore only a small contribution ($\approx 10\%$) comes from the interval $z_{\text{th}} \leqq z < z_{\min}$ where an exponential has been used to extrapolate the measured data.

In Fig. 12 the ratio r for mesons is plotted as a function of mass. The small error on r for ϕ-mesons from this experiment makes clear the distinction with baryons, where the value of r exceeds 2.5 [20, 23, 24]. This demonstrates that the baryon enhancement in Υ-decays is not a mass effect as predicted by cluster models [5].

Walsh and Peterson [8] have included in their model calculations of parton fragmentation the conjecture of Montvay [29] that the ϕ-meson, as a heavy isosinglet particle, is preferentially produced in gluon jets. They predict the ratio $r_\phi \geqq 1$, which is in contradiction with the experimental measurement $r_\phi = 1.32 \pm 0.08 \pm 0.09$. Since the enhancement for ϕ mesons is comparable to that of other mesons, our result excludes an enhanced production of isosinglet mesons in gluon jets over quark jets.

4 Conclusion

Using the ARGUS detector, a precision measurement of ϕ-meson spectra has been performed. The continuum results agree, within errors, with less precise data of other experiments. The predictions of the string and the parton shower model differ from the continuum data, but for direct Υ-decays, data and model calculations are in reasonable agreement. This difference is traced back to an excessively large branching ratio for the decay of charmed mesons into ϕ-mesons used in the models.

The ratio of the numbers of ϕ-mesons produced in direct $\Upsilon(1S)$- and $\Upsilon(2S)$-decays over that in continuum fragmentation is $r_\phi = 1.32 \pm 0.08 \pm 0.09$ and $r_\phi = 1.07 \pm 0.13 \pm 0.11$ respectively. These are similar to the values observed for other mesons. This result is in disagreement with model predictions. Specifically, parton shower models predict an increase of r with the meson mass [5]. Independent of any model predictions the observed constant value of r for mesons demonstrates that the increase of r detected for baryons is not a mass effect but rather a unique feature of baryon production.

Acknowledgement. It is a pleasure to thank U. Djuanda, E. Konrad, E. Michel and W. Reinsch for their competent technical help in running the experiment and processing the data. We thank Dr. H. Nesemann, B. Sarau and the DORIS group for the excellent operation of the storage ring. The visiting groups wish to thank the DESY directorate for the support and kind hospitality extended to them.

References

1. M. Althoff et al.: Z. Phys. C – Particles and Fields 17 (1983) 5; H. Aihara et al.: Phys. Rev. Lett. 52 (1984) 577; H. Albrecht et al.: Contributed paper to the XXXIInd International Conference on High Energy Physics, Leipzig 1984
2. Particle Data Group: Phys. Lett. 170 B (1986) 1
3. H. Aihara et al.: Phys. Rev. Lett. 53 (1984) 2378
4. B. Gittelman: Proc. XVI Intern. Symp. Multiparticle Dynamics 1985, p. 225. Kiryat 1985
5. R.D. Field: Proc. 1983 Intern. Symp. Lepton and Photon Interactions at High Energies, p. 593. Ithaca 1983; R.D. Field, Phys. Lett. 135 B (1984) 203
6. H. Albrecht et al.: Phys. Lett. 153 B (1985) 343
7. H. Albrecht et al.: Phys. Lett. 150 B (1985) 235
8. C. Peterson, T.F. Walsh: Phys. Lett. 91 B (1980) 455
9. H. Albrecht et al.: DESY 88-080, submitted to Nucl. Instr. Meth.
10. H. Gennow: SIMARG, Int. Rep. DESY-F15-85-02 (1985)
11. U. Matthiesen: PhD thesis, Dortmund, 1987
12. T. Sjöstrand: LU-TP 85-10 (1985), Lund
13. B. Andersson: Phys. Rep. C 97 (1983) 33
14. R. Barbieri et al.: Phys. Lett. 61 B (1976) 465
15. G.C. Fox, S. Wolfram: Nucl. Phys. B 168 (1980) 285; R.D. Field, S. Wolfram: Nucl. Phys. B 213 (1983) 65; T.D. Gottschalk: Nucl. Phys. B 214 (1983) 201; G. Marchesini, B.R. Webber: Nucl. Phys. B 238 (1984) 1
16. B.R. Webber: Nucl. Phys. B 238 (1984) 492

17. C.K. Ng: Phys. Rev. D 33 (1986) 3246
18. H. Scheck: PhD thesis, Dortmund, 1988
19. H. Yamamoto, Proc. 1985 Intern. Symp. Lepton and Photon Interactions at High Energies, p. 50. Kyoto 1985,
20. S. Behrends et al.: Phys. Rev. D 31 (1985) 2161
21. M. Derrick et al.: Phys. Rev. Lett. 54 (1985) 2568
22. H. Aihara et al.: Phys. Rev. Lett. 52 (1984) 2201
23. H. Albrecht et al.: Phys. Lett. 102 B (1981) 291
24. H. Albrecht et al.: DESY 87-141
25. W. Funk: Diplomarbeit, Heidelberg, 1988, IHEP-HD/88-3
26. A. Drescher: PhD thesis, Dortmund, 1987
27. S. Werner: Diplomarbeit, Heidelberg, 1987, IHEP-HD/87-1
28. A. Lindner: Diplomarbeit, Dortmund, 1988
29. I. Montvay: Phys. Lett. 84 B (1979) 331